

EXPERIMENTAL CALIBRATION OF NANOPARTICLE SINTERING SIMULATION

Obehi G Dibia*, Anil Yuksel*, Nilabh K Roy*, Chee S Foong†, Michael Cullinan*

*Department of Mechanical Engineering, University of Texas at Austin, Austin, TX 78712

†NXP Semiconductors, Austin, TX 78735

Abstract

Microscale Selective Laser Sintering models have been built as a basis to predict the properties of sintered nanoparticles under isothermal heating. These models use Phase Field Modelling (PFM) to track the diffusion of nanoparticles, resulting in properties such as the change in relative density and shrinkage of the sintered bed with time. To ensure the accuracy of these PFM models, experimental validation has to be done. This paper presents the experimental procedure and results for isothermally heating nanoparticles up to 450 – 600°C, at sintering times varying from 1 to 45 minutes. Measurement uncertainties are calculated from deviations in calculating the density. Experimental results from this process are then used to calibrate the simulation to determine the number of simulation timesteps which correspond to a minute of physical time. The calibration constant derived is then used to map simulation constants to physical constants. These constants are later compared to bulk properties.

Introduction

Microscale Selective Laser Sintering is a promising process which looks at the creation of sub-micrometer parts through the sintering of nanoparticles [1]. These nanoparticles fuse together using energy absorbed from a laser source. With the development of this process, there is a concurrent need for models able to predict properties of sintered parts. One such model is presented in [2] and looks at the changes in the rate of densification and shrinkage during sintering. The simulation presented in this model uses Phase Field Modelling to track the diffusion of a large number of particles, 43 particles in a 1 by 1 micrometer bed, and 134 particles in a 2 by 2 micrometer bed. The simulations in this paper look at an isothermally heated bed with simulation parameters which are set constant for all particles in the bed. These simulation parameters are temperature dependent, as such, they need to be calibrated against experimental data, to map simulation constants to corresponding physical temperatures. Copper nanoparticles were chosen for the initial calibration of these simulation constants.

Metal nanoparticles such as silver, gold and copper have been studied in recent years due to the high electrical conductivity of these materials [3]. However, most of the sintering experiments carried out for these particles center around measuring electrical conductivity [4,5]. Few researchers have looked into measuring changes in relative density of sintered nanoparticles. Wang et al, studied the densification of Beryllium oxide nanoparticle powders, finding that these particles began to sinter at temperatures lower than the conventional sintering temperatures [6]. There have been no studies done on the densification of isothermally heated nanoparticle inks. This study shows densification results for the sintering of copper nanoparticles. The experiments are carried out by changing heating times and temperatures. The relative change in density curve

is determined from analyzing these experiments, and the curve fit is then calibrated against the relative density curve fit from simulations.

Experiments

Sintering experiments were carried out on copper nanoparticle inks from Intrinsic [7]. The first step of the experimental procedure involved drying out the ink. 2ml of copper nanoparticle ink was dispensed into a glass petri dish using a rubber pipette. The petri dish of ink was dried on a hot plate at around 95°C for 16 hours. After the solvent in the ink dries off, dried copper flakes of coated nanoparticles are scraped off the petri dish with a flat spatula. These dried flakes are then put into crucibles. Pressure is applied to form the flakes into pellets in the crucibles. These crucibles are put into a furnace and subject to isothermal heating. In the furnace, the coating around the particles dry off and the nanoparticles sinter together into a solid pellet. The flow of the experimental procedure is shown in the images in Figure 1. The sintering experiments were carried out under flowing Argon and Hydrogen to control oxidation of the copper nanoparticles. The ratio of Argon to Hydrogen gas flow is 300:100.

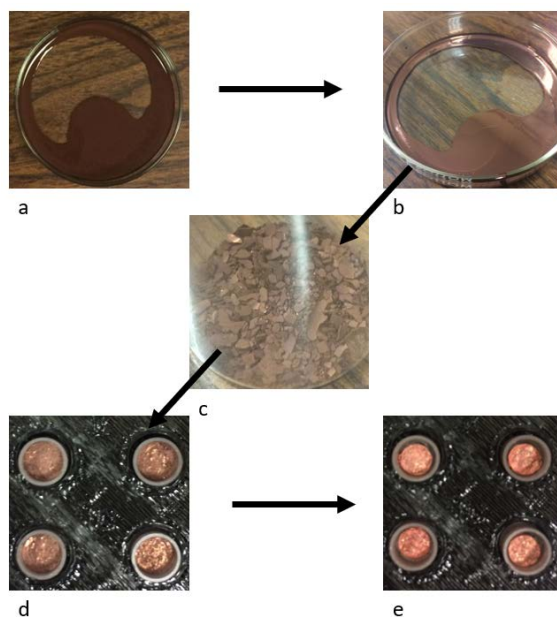


Figure 1. Experimental procedure. a. Copper nanoparticle ink. b. Dried ink. c. Scraped off dried flakes. d. Pellets in crucible before sintering. e. Pellets in crucible after sintering

SEM images were taken of the flakes before sintering, and the pellets after sintering. These images in Figure 2, show that before sintering the particles are discrete and can be seen separate from each other. After sintering, the images of the pellets show that necks have formed between the nanoparticles after heating.

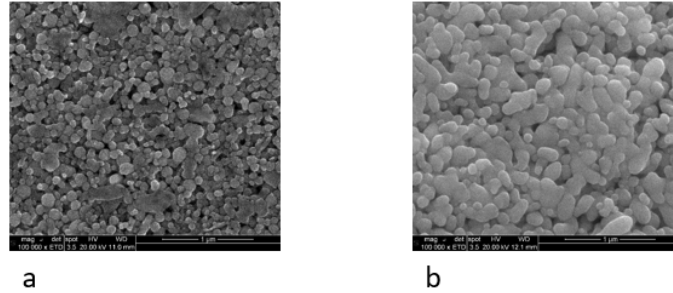


Figure 2. SEM Images of sintered nanoparticles. a. Before sintering. b. After sintering

After the experiments were done density measurements were taken. The density measurement is calculated as the ratio of mass to volume. The mass was measured using a digital weight scale. The volume was calculated from the measured height of the pellets. The height measurements were taken from the deflection of stoppers. A plastic stopper was put into the empty crucible and the deflection of the stopper was measured. The height of the pellet was calculated from the difference between the stopper deflections between the empty crucible and the deflections with the pellet in the crucible. The relative density was calculated from the density measurements using Eqn 1.

$$\rho_{rel} = \frac{\rho_i - \rho_o}{\rho_i} \quad Eqn. 1$$

Where ρ_o is the initial density and ρ_i is the final density.

The sintering experiments were carried out at 450, 500, 550 and 600°C and the relative density data at these temperatures were fit to an expression of the form in Eqn 2. This form of the equation was modified from [8] where the diffusion coefficient follows an exponential decay fit similar to Eqn. 2.

$$\rho_{rel} = K_1 e^{-\frac{K_2}{t+K_3}+K_4} + K_5 \quad Eqn. 2$$

A plot of the experiment data points and the best fit curve for the decay in Eqn. 2 is shown in Figure 3. A consolidation of all these plots is shown in Figure 4. From Figure 3, it can be seen that sintering is characterized by an initial rate of rapid densification and as the sintering time proceeds the rate of densification approaches a steady state value. Figure 4 shows that as the temperature increases, the amount of time it takes for the relative density to reach steady state decreases. These curves from the experiments were set against the results from the simulation and the appropriate simulation constants and simulation time calibration constant were calculated. The process of deriving this is discussed next.

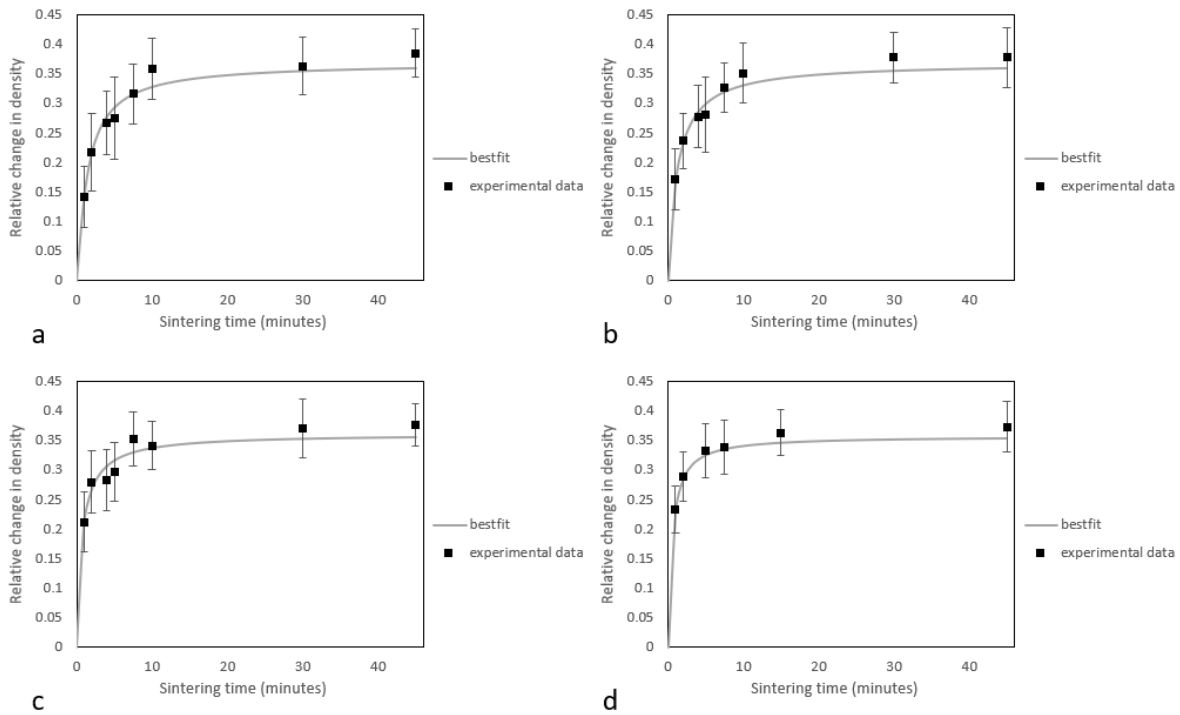


Figure 3. Experimental data and curve fit at a. 450°C. b. 500°C. c. 550°C. d. 600°C

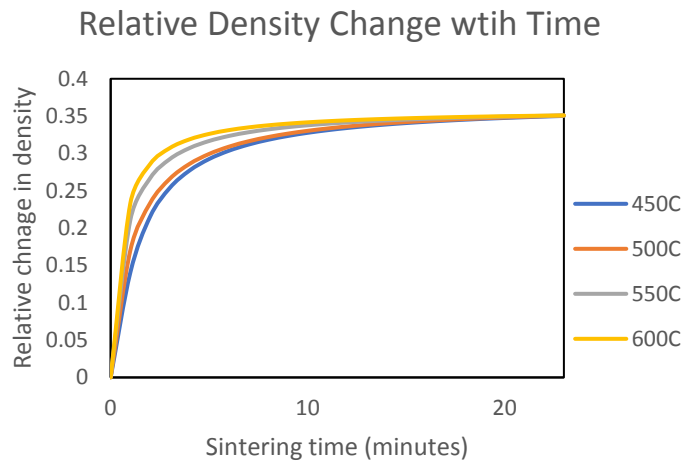


Figure 4. Consolidation of experiment fit plots

Simulation Calibration

The Phase Field Simulation (PFM) in [2] gives results for the diffusion of nanoparticles in a powder bed. The beds are generated using a bed generation simulation [9] to match actual physical beds. An initial configuration of a powder bed is shown in Figure 5.

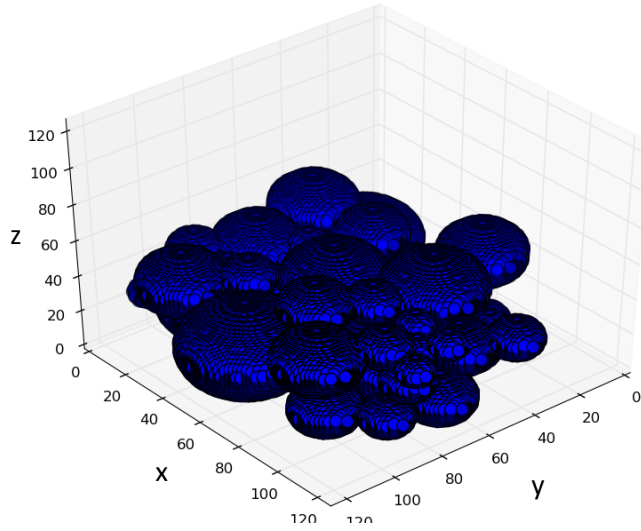


Figure 5. Initial Powder Bed Configuration

Previous results in the PFM diffusion simulation show that the process of sintering is characterized by an initial stage of neck formation between particles in contact. After the neck forms, the diffusion process shows neck growth and grain boundary migration. The analysis in these simulations were done on a center box of the simulation bed, to make the data collated impervious to edge effects. This process of diffusion in the center of the bed is shown in the images in Figure 6.

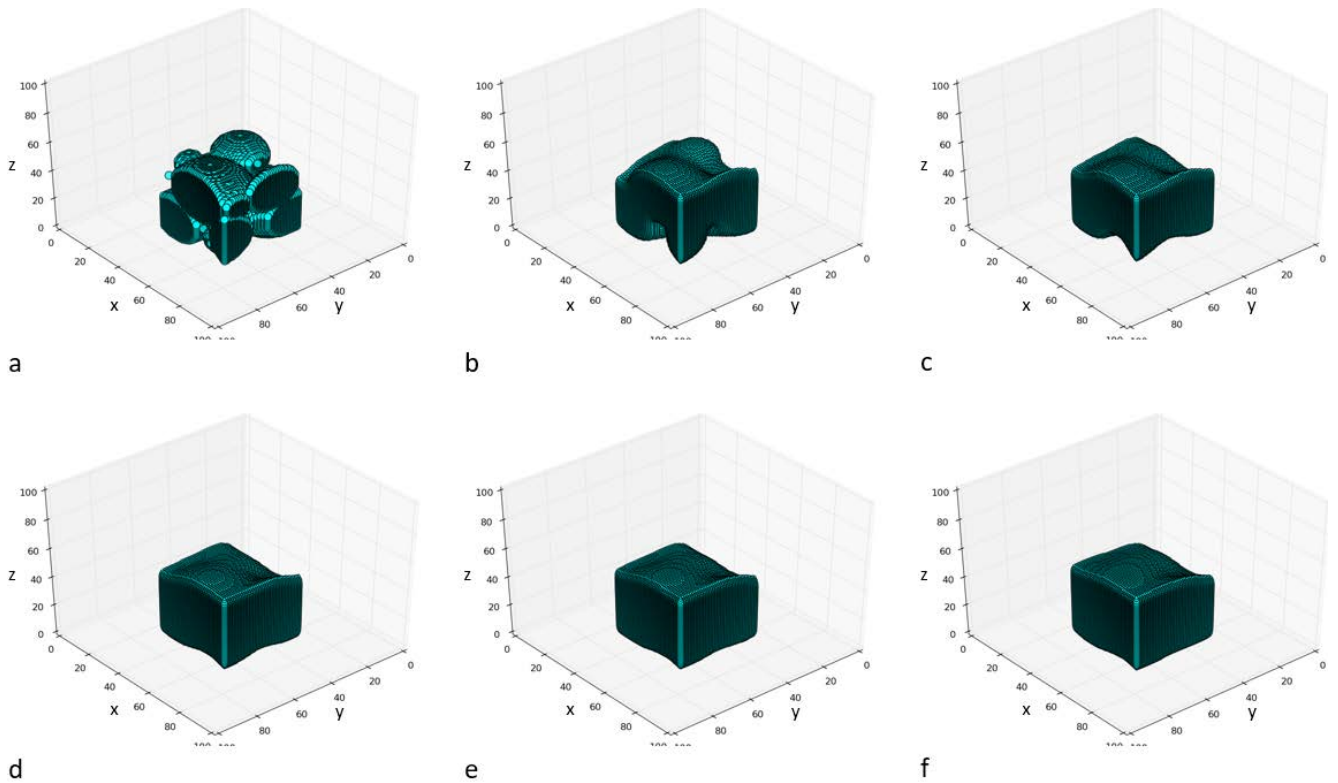


Figure 6. Densification in the center of the simulation bed after a. 0 timesteps. b. 80000 timesteps. c. 160000 timesteps. d. 480000 timesteps. e. 1200000 timesteps. f. 2400000 timesteps

The relative density of these beds was calculated similar to the experiments using Eqn. 1. The results from the relative density calculation is shown in Figure 7. The error bounds in this calculation is derived from looking at the deviation in the relative density measurements as a result of changing the location of the analysis box in the center of the simulation. The trend in the relative density curve in Figure 7 matches the trend seen in the experiment curves where sintering is characterized by a fast rate of densification which slows down to steady state with simulation time.

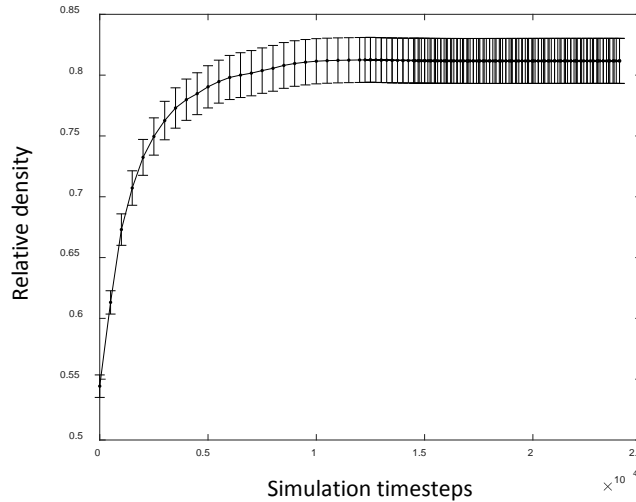


Figure 7. Relative density curve from simulations

The rate of densification in this simulation are set by the temperature dependent constants. These constants are gradient terms related to surface energy, β_ρ , and grain boundary energy, β_η , coefficients as well as the diffusion constants, surface D_{surf} , grain boundary, D_{gb} , and volume D_{vol} . These constants were changed to get the closest fit for the simulation density curve to the experiments curve for each temperature. The time calibration constant, A , is defined as in Eqn. 3.

$$t_{exp}(min) = \frac{t_{sim}(timesteps)}{A} \quad Eqn. 3$$

A defines the number of simulation timesteps that corresponds to time in minutes. This constant is determined using a bracketing algorithm that converges to the value of A which minimizes the error between the simulation results and the experiment results. The results fitting the simulation to experiments are shown in Figure 8.

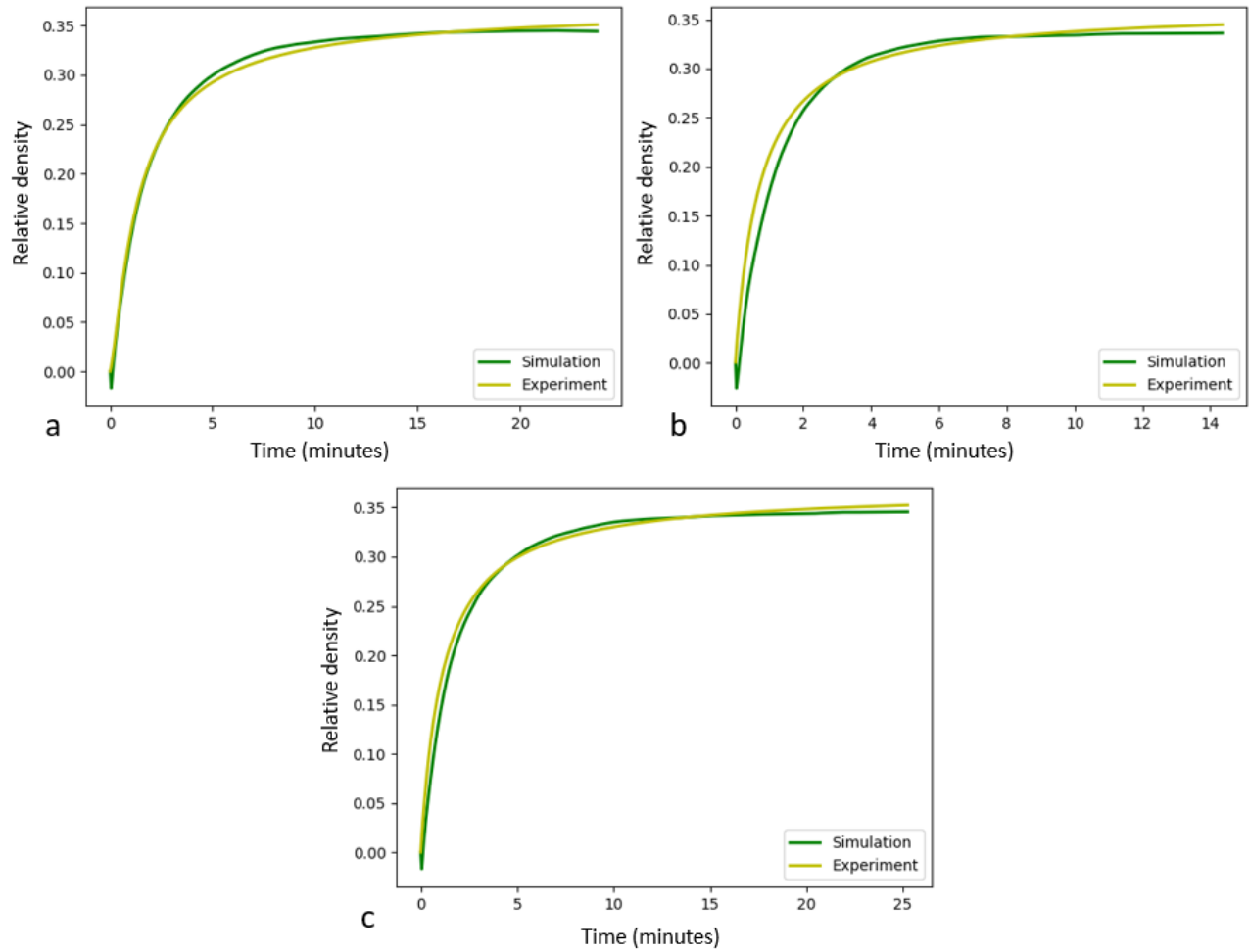


Figure 8. Comparing experimental fit to simulations for a. 450°C. b. 500°C. c. 550°C.

The results for the time calibration values are shown in Table 1. The Table shows the results for the range and averages of the error and time calibration values. The range included in these values, like the error bars in Figure 6, are a result of carrying out the calibration analysis on different boxes in the center of the simulation bed. The data in Table 1 shows an overall average error of about 9% between the simulation and experiments. The time calibration factor shown in the table has an average of 20% deviation between each temperature.

Table 1. Calibration Results: Time and Error

	Time Calibration, A (timesteps/minute)			Error (%)		
	Minimum	Maximum	Average	Minimum	Maximum	Average
450°C	101070	388864	215319	3.22	30.14	13.54
500°C	57644	277293	167598	3.57	10.91	7.01
550°C	71110	383773	250102	3.99	9.79	6.76

Once calculated, the time dependent simulation constants were mapped to constants with actual physical meanings. The diffusion constants were mapped using Eqn. 4.

$$D_{sim} \left(\frac{\text{pixels}^2}{\text{timesteps}} \right) \Rightarrow \frac{D_{sim} A}{60 S^2} \Rightarrow D_{actl} \left(\frac{\text{cm}^2}{\text{s}} \right) \quad \text{Eqn. 4}$$

Where D_{sim} represents the simulation diffusion coefficients and D_{actl} represents the diffusion coefficients when mapped to the corresponding units in a CGS system. A is the time calibration constant in Eqn. 3 having units of timesteps/minute and S is the size calibration constant. S here is set as 944822 pixels/cm. The values used for the diffusion constants in the simulation were mapped to physical units and are shown in Table 2. Surface, grain boundary and volume diffusion coefficients in the simulation follow the ratio 1000:100:1 respectively.

Table 2. Calibration Results: Diffusion constants

	Surface Diffusion coefficients (cm ² /s)	
	Average	Uncertainty
450°C	2E-07	1E-07
500°C	2.2E-07	7.9E-08
550°C	3E-07	1E-07

The diffusion constants used in the simulations at 500°C were compared to bulk measurements from literature. As of this point there has been no experimentally determined surface diffusion coefficients for copper nanoparticles to compare against the constants in Table 2. Bonzel and Gjostein [10] found that at 500°C the surface diffusion coefficient of bulk copper is 1.91E-07 cm²/s. This value falls within the same order of magnitude as the value obtained from the simulations. Additionally, since the ratio of surface area to volume is higher for nanoparticles, the surface diffusion coefficient for nanoparticles is expected to be higher than that for bulk, which is in agreement with the results presented. This comparison is further validation of the model.

Future Work

Given the simulation work and experiments carried out to calibrate the simulation, the next step is to quantify the error in the simulation. As shown in the uncertainty in changing the position of the analysis box, there is a significant amount of error that comes with the configuration of the particles in the bed. To completely quantify this uncertainty, different simulation beds have to be tested to determine the changes in calibration constants and rate of densification with changing the initial configuration of the bed. Next, given the map of simulation constants to physical temperature, the simulation would have to be transitioned to include transient heating more representative of a temperature gradient. This temperature gradient is important because in a typical laser sintering process, there is a temperature difference between the particles in the laser irradiated spot and the surrounding particles outside the laser heating zone. Also, the simulation has to be transitioned to include multiple layers. This would enable the study of the effects that the interaction between layers has on the properties of the sintered bed.

Conclusion

This paper presents densification results which were derived from isothermal heating of copper nanoparticles. The data shows that after 10 minutes of heating at 450°C the density value starts to reach the maximum steady state value. As heating temperature increases, the amount of time the nanoparticles take to reach steady state decreases. The densification curves obtained from the experimental data are calibrated to match sintering simulation results and it is seen that the simulation trend is in good agreement with the experimental data. The diffusion constants are mapped to physical units and are compared to bulk properties from literature. This comparison shows that the surface diffusion coefficient is higher for the copper nanoparticles than those reported for bulk copper.

Acknowledgements

This material is based upon work supported by the National Science Foundation under Grant No. **1728313**. The authors would like to acknowledge Texas Advanced Computing Center (TACC) for the Supercomputing resources, and NXP Semiconductors for the financial support provided.

References

- [1] Roy, N. K., Foong, C. S., and Cullinan, M. A., 2016, "Design of a Micro-scale Selective Laser Sintering System," 2016 Annual International Solid Freeform Fabrication Symposium.
- [2] Dibua, O. G., Yuksel, A., Roy, N. K., Foong, C. S., and Cullinan, M., 2017, "Modelling Nanoparticle Sintering in a Microscale Selective Laser Sintering Process," 2018 Annual International Solid Freeform Fabrication Symposium.
- [3] Khondoker, M. A. H., Mun, S. C., and Kim, J., 2013, "Syntheses and Characterization of Conductive Silver Ink for Electrode Printing on Cellulose Film," *Applied Physics A: Materials Science & Processing*, **112**, pp. 411-418.
- [4] Kumpulainen, T., Pekkanen, J., Valkama, J., Laakso, J., Tuokko, R., and Mantysalo, M., 2011, "Low temperature nanoparticle sintering with continuous wave and pulse lasers," *Optics & Laser Technology*, **43**, pp. 570-576.
- [5] Halonen, E., Viiru, T., Ostman, K., Cabezas, A. L., and Mantysalo, M., 2013, "Oven Sintering Process Optimization for Inkjet-Printed Ag Nanoparticle Ink," *IEEE Transactions on Components, Packaging and Manufacturing Technology*, **3**, pp. 350-356.
- [6] Wang, X., Wang, R., Peng, C., Li, T., and Liu, B., 2010, "Synthesis and sintering of beryllium oxide nanoparticles," *Progress in Natural Science: Materials International*, **20**, pp. 81-86.
- [7] n.d. "CI-005_Data_Sheet_2017," Intrinsic Materials.
- [8] Martin, C. L., Schneider, L. C. R., Olmos, L., and Bouvard, D., 2006, "Discrete element modeling of metallic powder sintering," *Scripta Materialia*, **55**, pp. 425-428.
- [9] Yuksel, A., and Cullinan, M., 2016, "Modeling of nanoparticle agglomeration and powder bed formation in microscale selective laser sintering systems," *Additive Manufacturing*, **12**, pp. 204-215.

- [10] Hoehne, K., and Sizmann, R., 1971, "Volume and Surface Self-Diffusion Measurements on Copper by Thermal Surface Smoothing," *Physica Status Solidi*, **5**, pp. 577-588.